

Example 4-4

Calculate the pressure difference, i.e., capillary pressure, and capillary rise in an oil-water system from the following data:

$$\theta = 30^\circ \quad \rho_w = 1.0 \text{ gm/cm}^3 \quad \rho_o = 0.75 \text{ gm/cm}^3$$

$$r = 10^{-4} \text{ cm} \quad \sigma_{ow} = 25 \text{ dynes/cm}$$

Solution

Step 1. Apply Equation 4-32 to give

$$p_c = \frac{(2)(25)(\cos 30^\circ)}{0.0001} = 4.33 \times 10^5 \text{ dynes/cm}^2$$

Since $1 \text{ dynes/cm}^2 = 1.45 \times 10^5 \text{ psi}$, then

$$p_c = 6.28 \text{ psi}$$

This result indicates that the oil-phase pressure is 6.28 psi higher than the water-phase pressure.

Step 2. Calculate the capillary rise by applying Equation 4-33.

$$h = \frac{(2)(25)(\cos 30^\circ)}{(0.0001)(980.7)(1.0 - 0.75)} = 1766 \text{ cm} = 75.9 \text{ ft}$$

Capillary Pressure of Reservoir Rocks

The interfacial phenomena described above for a single capillary tube also exist when bundles of interconnected capillaries of varying sizes exist in a porous medium. The capillary pressure that exists within a porous medium between two immiscible phases is a function of the interfacial tensions and the average size of the capillaries, which, in turn, control the curvature of the interface. In addition, the curvature is also a function of the saturation distribution of the fluids involved.

Laboratory experiments have been developed to simulate the displacing forces in a reservoir in order to determine the magnitude of the capillary forces in a reservoir and, thereby, determine the fluid saturation distributions and connate water saturation. One such experiment is called the *restored capillary pressure technique*, which was developed primarily to determine the magnitude of the *connate water saturation*. A diagrammatic sketch of this equipment is shown in Figure 4-4.

Briefly, this procedure consists of *saturation a core 100%* with the *reservoir water* and then *placing the core on a porous membrane*, which is saturated 100% with water and is permeable to the water only, under the pressure drops imposed during the experiment. Air is then *admitted* into the core chamber and the pressure is increased until a *small amount* of water is displaced through the porous, semi-permeable membrane into the graduated cylinder. *Pressure is held*

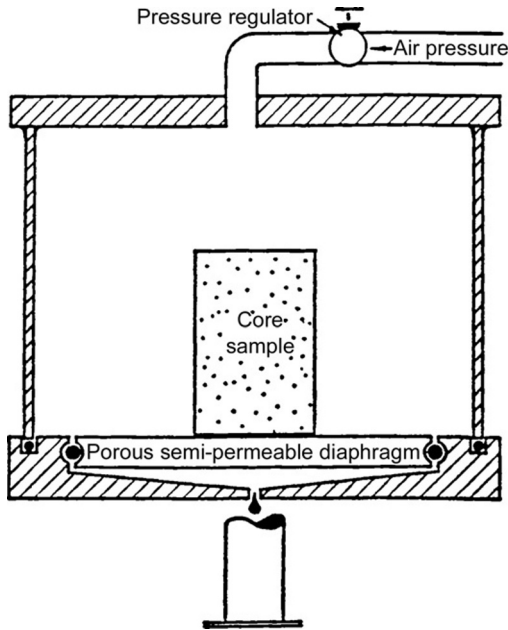


FIGURE 4-4 Capillary pressure equipment. (After Cole, F., 1969).

constant until no more water is displaced, which may require several days or even several weeks, after which the core is removed from the apparatus and the water saturation determined by weighing. The core is then replaced in the apparatus, the pressure is increased, and the procedure is repeated until the water saturation is reduced to a minimum.

The data from such an experiment are shown in Figure 4-5. Since the pressure required to displace the wetting phase from the core is exactly equal to the capillary forces holding the remaining water within the core after equilibrium has been reached, the pressure data can be plotted as capillary pressure data. Two important phenomena can be observed in Figure 4-5. First, there is a finite capillary pressure at 100% water saturation that is necessary to force the nonwetting phase into a capillary filled with the wetting phase. This minimum capillary pressure is known as the displacement pressure, p_d .

If the largest capillary opening is considered as circular with a radius of r , the pressure needed for forcing the nonwetting fluid out of the core is:

$$p_c = \frac{2\sigma(\cos \theta)}{r}$$

This is the minimum pressure that is required to displace the wetting phase from the largest capillary pore because any capillary of smaller radius will require a higher pressure.

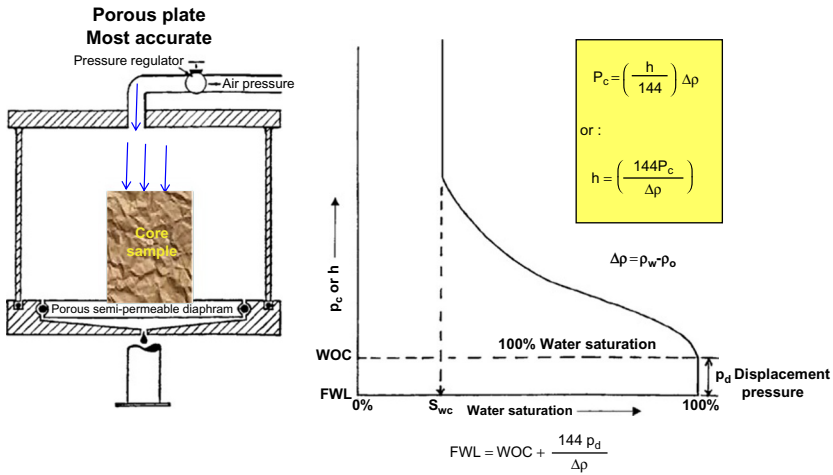


FIGURE 4-5 Capillary pressure curve.

As the wetting phase is displaced, the second phenomenon of any **immiscible displacement process** is encountered, that is, the reaching of some finite minimum irreducible saturation. This irreducible water saturation is referred to as **connate water**.

It is possible from the capillary pressure curve to calculate the average **size of the pores** making up a stated fraction of the total pore space. Let p_c be the average capillary pressure for the 10% between saturation of 40 and 50%. The average capillary radius is obtained from

$$r = \frac{2\sigma(\cos \theta)}{P_c}$$

The above equation may be solved for r providing that the interfacial tension σ , and the angle of contact θ may be evaluated.

Figure 4-6 is an example of typical oil-water capillary pressure curves. In this case, **capillary pressure is plotted versus water saturation for four rock samples with permeabilities increasing from k_1 to k_4** . It can be seen that, for decreases in permeability, there are corresponding increases in capillary pressure at a constant value of water saturation. This is a reflection of the influence of pore size since the smaller diameter pores will invariably have the lower permeabilities. Also, as would be expected the **capillary pressure for any sample increases with decreasing water saturation**, another indication of the effect of the radius of curvature of the water-oil interface.

Capillary Hysteresis

It is generally agreed that the pore spaces of reservoir rocks were originally filled with water, after which **oil moved into the reservoir, displacing** some

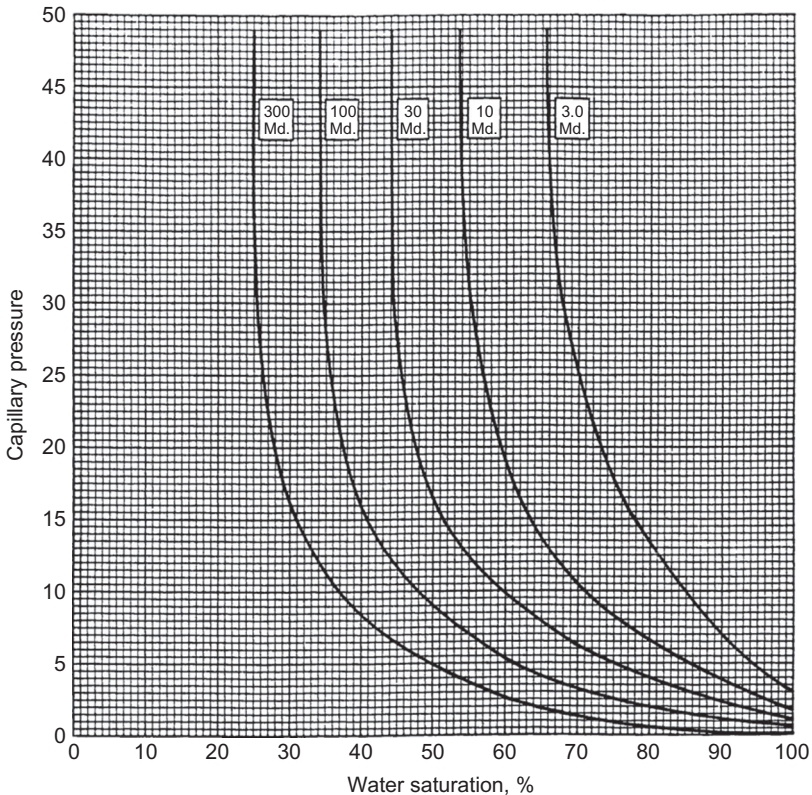


FIGURE 4-6 Variation of capillary pressure with permeability.

of the water and reducing the **water to some residual saturation**. When discovered, the reservoir pore spaces are filled with a connate-water saturation and an oil saturation. All laboratory experiments are designed to duplicate the saturation history of the reservoir. The process of generating the capillary pressure curve by **displacing the wetting phase, i.e., water, with the nonwetting phase (such as with gas or oil)**, is called the **drainage process**.

This drainage process establishes the fluid saturations, which are found when the reservoir is discovered. The other principal flow process of interest involves reversing the drainage process by **displacing the nonwetting phase (such as with oil) with the wetting phase, (e.g., water)**. This displacing process is termed the **imbibition process** and the resulting curve is termed the **capillary pressure imbibition curve**. The process of **saturation and desaturation** a core with the nonwetting phase is called **capillary hysteresis**. Figure 4-7 shows typical drainage and imbibition capillary pressure curves. The two capillary pressure-saturation curves are not the same.

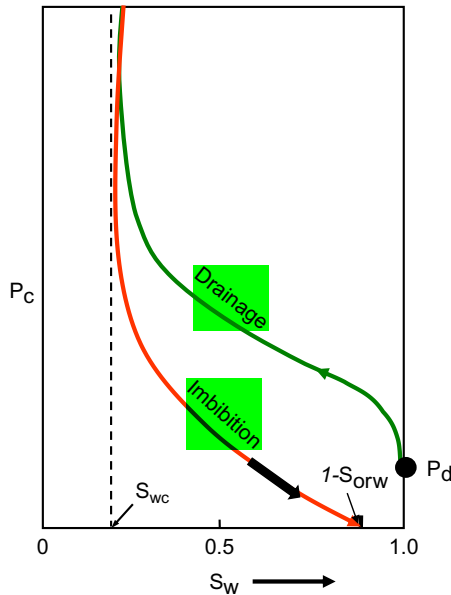


FIGURE 4-7 Capillary pressure hysteresis.

This difference in the saturating and desaturating of the capillary-pressure curves is closely related to the fact that the advancing and receding contact angles of fluid interfaces on solids are different. Frequently, in natural crude oil-brine systems, **the contact angle or wettability may change with time.** Thus, if a rock sample that has been thoroughly cleaned with volatile solvents is exposed to crude oil for a period of time, it will behave as though it were oil wet. But if it is exposed to brine after cleaning, it will appear water wet. At the present time, one of the greatest unsolved problems in the petroleum industry is that of wettability of reservoir rock.

Another mechanism that has been proposed by [McCardell \(1955\)](#) to account for capillary hysteresis is called the *ink-bottle effect*. This phenomenon can be easily observed in a capillary tube having variations in radius along its length. Consider a capillary tube of axial symmetry having roughly sinusoidal variations in radius. When such a tube has its lower end immersed in water, the water will rise in the tube until the hydrostatic fluid head in the tube becomes equal to the capillary pressure. If then the tube is lifted to a higher level in the water, some water will drain out, establishing a new equilibrium level in the tube.

When the meniscus is advancing and it approaches a constriction, it *jumps* through the neck, whereas when receding, it halts without passing through the neck. This phenomenon explains why a given capillary pressure corresponds to a higher saturation on the drainage curve than on the imbibition curve.

Initial Saturation Distribution in a Reservoir

An important application of the concept of capillary pressures pertains to the fluid distribution in a reservoir prior to its exploitation. The capillary pressure-saturation data can be converted into height-saturation data by arranging Equation 4-29 and solving for the height **h above the freewater level**.

$$h = \frac{144 p_c}{\Delta \rho} \tag{4-34}$$

where

p_c = capillary pressure, psia

$\Delta \rho$ = density difference between the wetting and nonwetting phase, lb/ft³

H = height above the free-water level, ft

Figure 4-8 shows a plot of the water saturation distribution as a function of distance from the free-water level in an **oil-water system**.

It is essential at this point to introduce and define four important concepts:

- o **Transition zone**
- o **Water-oil contact (WOC)**
- o **Gas-oil contact (GOC)**
- o **Free water level (FWL)**

Figure 4-9 illustrates an **idealized gas, oil, and water distribution** in a reservoir. The figure indicates that the saturations are gradually changing from 100% water in the water zone to irreducible water saturation some vertical distance above the water zone. This vertical area is referred to as the *transition zone*, which must exist in any reservoir where there is a bottom water table. The

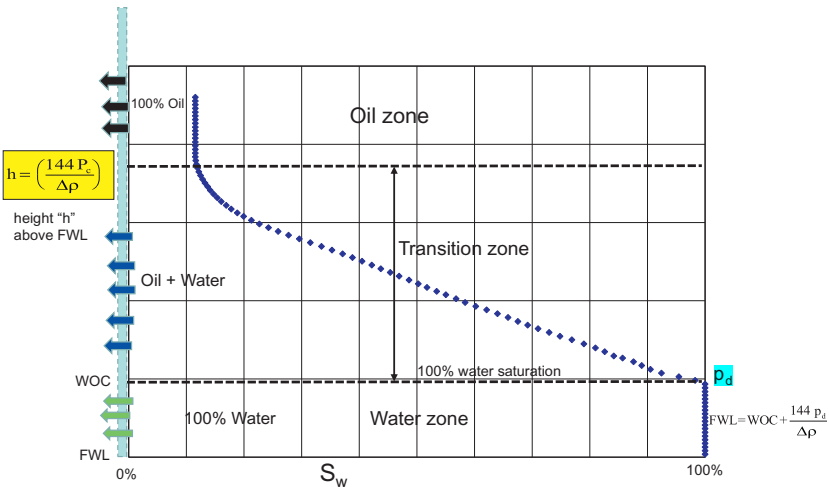


FIGURE 4-8 Water saturation profile.

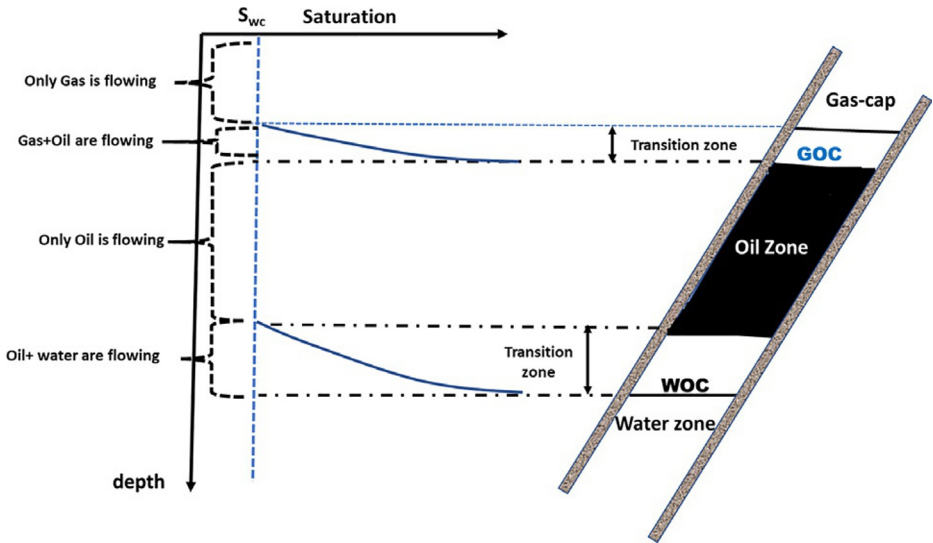


FIGURE 4-9 Initial saturation profile in a combination-drive reservoir.

transition zone is then defined as the vertical thickness over which the water saturation ranges from 100% saturation to irreducible water saturation S_{wc} . The important concept to be gained from Figure 4-9 is that there is no abrupt change from 100% water to maximum oil saturation. The creation of the oil-water transition zone is one of the major effects of capillary forces in a petroleum reservoir.

Similarly, the total liquid saturation (i.e., oil and water) is smoothly changing from 100% in the oil zone to the connate water saturation in the gas cap zone. A similar transition exists between the oil and gas zone. Figure 4-8 serves as a definition of what is meant by gas-oil and water-oil contacts. The WOC is defined as the "uppermost depth in the reservoir where a 100% water saturation exists." The GOC is defined as the "minimum depth at which a 100% liquid, i.e., oil + water, saturation exists in the reservoir."

Section A of Figure 4-10 shows a schematic illustration of a core that is represented by five different pore sizes and completely saturated with water, i.e., wetting phase. Assume that we subject the core to oil (the nonwetting phase) with increasing pressure until some water is displaced from the core, i.e., displacement pressure p_d . This water displacement will occur from the largest pore size. The oil pressure will have to increase to displace the water in the second largest pore. This sequential process is shown in sections B and C of Figure 4-10.

It should be noted that there is a difference between the free water level (FWL) and the depth at which 100% water saturation exists. From a reservoir engineering standpoint, the free water level is defined by zero capillary pressure. Obviously, if the largest pore is so large that there is no capillary rise

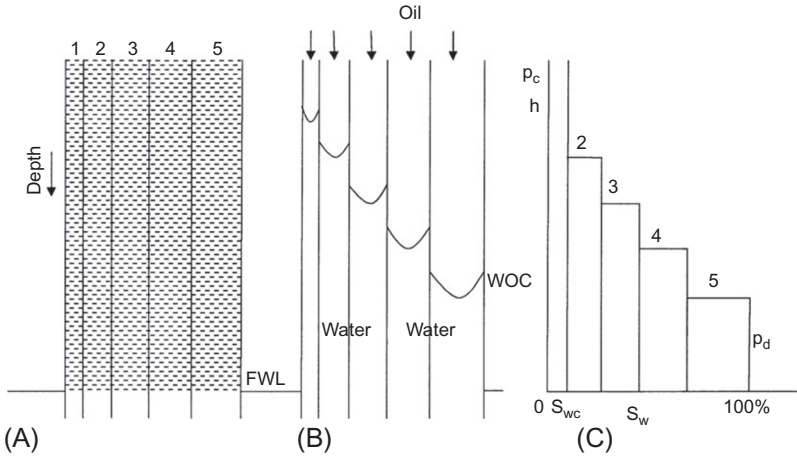


FIGURE 4-10 Relationship between saturation profile and pore-size distribution.

in this **size pore**, then the **free water level and 100% water saturation level, i.e., WOC**, will be the same. This concept can be expressed mathematically by the following relationship:

$$FWL = WOC + \frac{144 p_d}{\Delta \rho} \tag{4-35}$$

where

- p_d = displacement pressure, psi
- $\Delta \rho$ = density difference, lb/ft³
- FWL = free water level, ft
- WOC = water-oil contact, ft

Example 4-5

The reservoir capillary pressure-saturation data of the Big Butte Oil reservoir is shown graphically in **Figure 4-11**. Geophysical log interpretations and core analysis establish the **WOC at 5023 ft**. The following additional data are available:

- Oil density = 43.5 lb/ft³
- Water density = 64.1 lb/ft³
- Interfacial tension = 50 dynes/cm

Calculate:

- Connate water saturation (S_{wc})
- Depth to FWL
- Thickness of the transition zone
- Depth to reach 50% water saturation

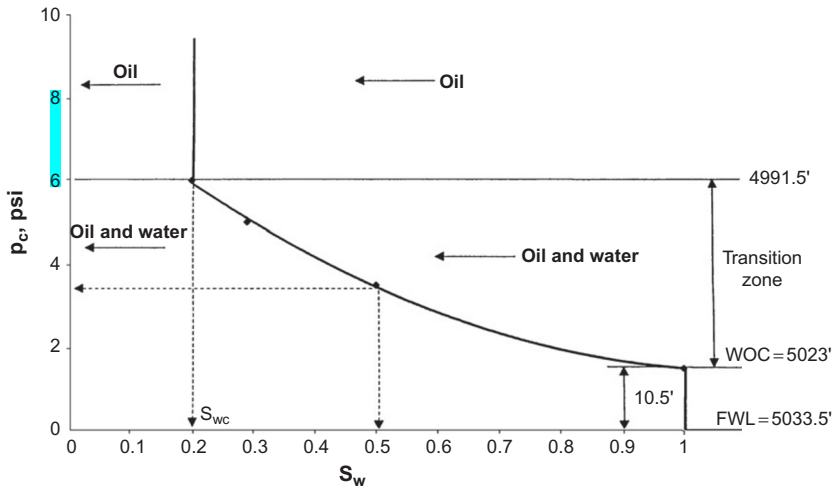


FIGURE 4-11 Capillary pressure saturation data.

Solution

- From Figure 4-11, connate-water saturation is 20%.
- Applying Equation 4-35 with a displacement pressure of 1.5 psi gives

$$\text{FWL} = 5,023 + \frac{(144)(1.5)}{(64.1 - 43.5)} = 5,033.5 \text{ ft}$$

- Thickness of transition zone = $\frac{144(6.0 - 1.5)}{(64.1 - 43.5)} = 31.5 \text{ ft}$

- P_c at 50% water saturation = 3.5 psia

$$\text{Equivalent height above the FWL} = (144)(3.5)/(64.1 - 43.5) = 24.5 \text{ ft}$$

$$\text{Depth to 50\% water saturation} = 5,033.5 - 24.5 = 5,009 \text{ ft}$$

The above example indicates that only oil will flow in the interval between the top of the pay zone and depth of 4,991.5 ft. In the transition zone, i.e., the interval from 4,991.5 ft to the WOC, oil production would be accompanied by simultaneous water production.

It should be pointed out that the thickness of the transition zone may range from few feet to several hundred feet in some reservoirs. Recalling the capillary rise equation, i.e., height above FWL,

$$h = \frac{2\sigma(\cos\phi)}{r_g \Delta\rho}$$

The above relationship suggests that the height above FWL increases with decreasing the density difference $\Delta\rho$.

From a practical standpoint, this means that in a gas reservoir having a gas-water contact, the thickness of the transition zone will be a minimum since $\Delta\rho$ will be large. Also, if all other factors remain unchanged, a low API gravity oil reservoir with an oil-water contact will have a longer transition zone than a high API gravity oil reservoir. Cole (1969) illustrated this concept graphically in Figure 4-12.

The above expression also shows that as the radius of the pore r increases the volume of h decreases. Therefore, a reservoir rock system with small pore sizes will have a longer transition zone than a reservoir rock system comprised of large pore sizes.

The reservoir pore size can often be related approximately to permeability, and where this applies, it can be stated that high permeability reservoirs will have shorter transition zones than low permeability reservoirs as shown graphically in Figure 4-13. As shown by Cole (Figure 4-14), a tilted water-oil contact could be caused by a change in permeability across the reservoir. It should be emphasized that the factor responsible for this change in the location of the water-oil contact is actually a change in the size of the pores in the reservoir rock system.

The previous discussion of capillary forces in reservoir rocks has assumed that the reservoir pore sizes, i.e., permeabilities, are essentially uniform. Cole (1969) discussed the effect of reservoir non-uniformity on the distribution of the fluid saturation through the formation. Figure 4-15 shows a hypothetical reservoir rock system that is comprised of seven layers. In addition, the seven layers are characterized by only two different pore sizes, i.e., permeabilities, and corresponding capillary pressure curves as shown in section A of Figure 4-15. The resulting capillary pressure curve for the layered reservoir would resemble that

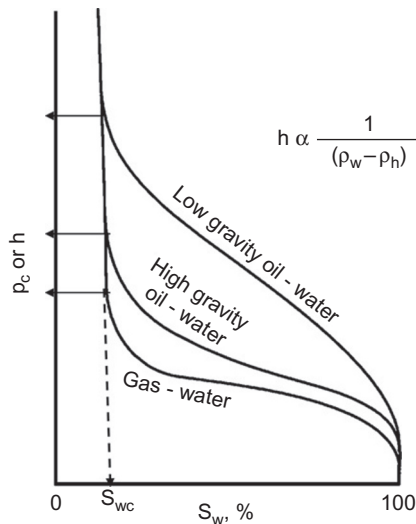


FIGURE 4-12 Variation of transition zone with hydrocarbon gravity.

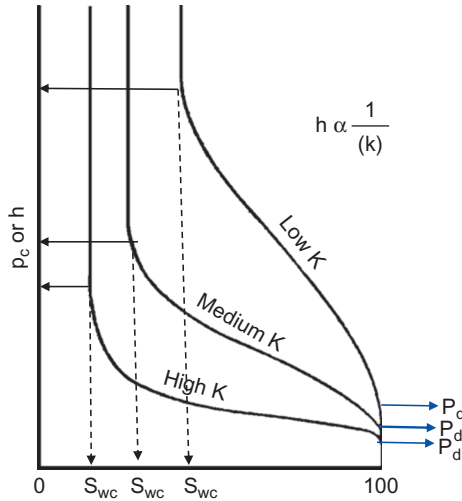


FIGURE 4-13 Variation of transition zone with absolute permeability.

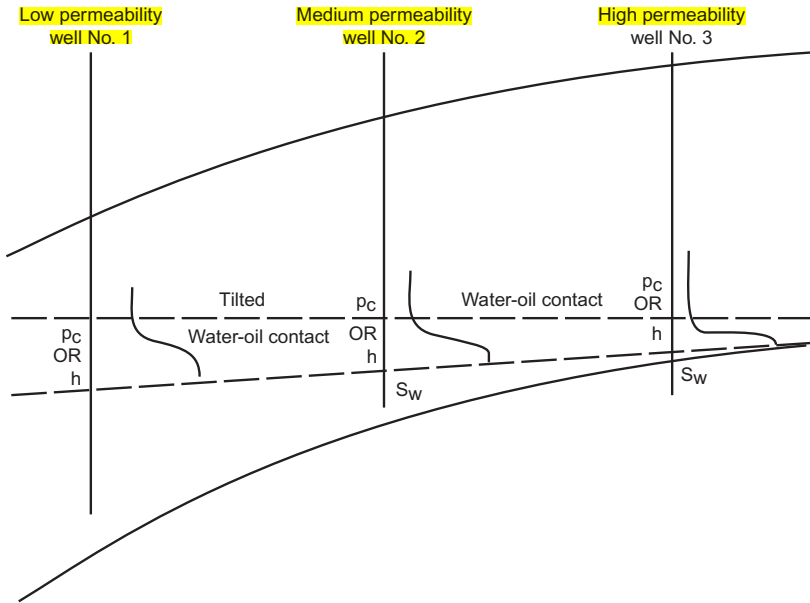


FIGURE 4-14 Tilted WOC. (After Cole, F., 1969).

shown in section B of Figure 4-15. If a well were drilled at the point shown in section B of Figure 4-15, Layers 1 and 3 would not produce water, while Layer 2, which is above Layer 3, would produce water since it is located in the transition zone.

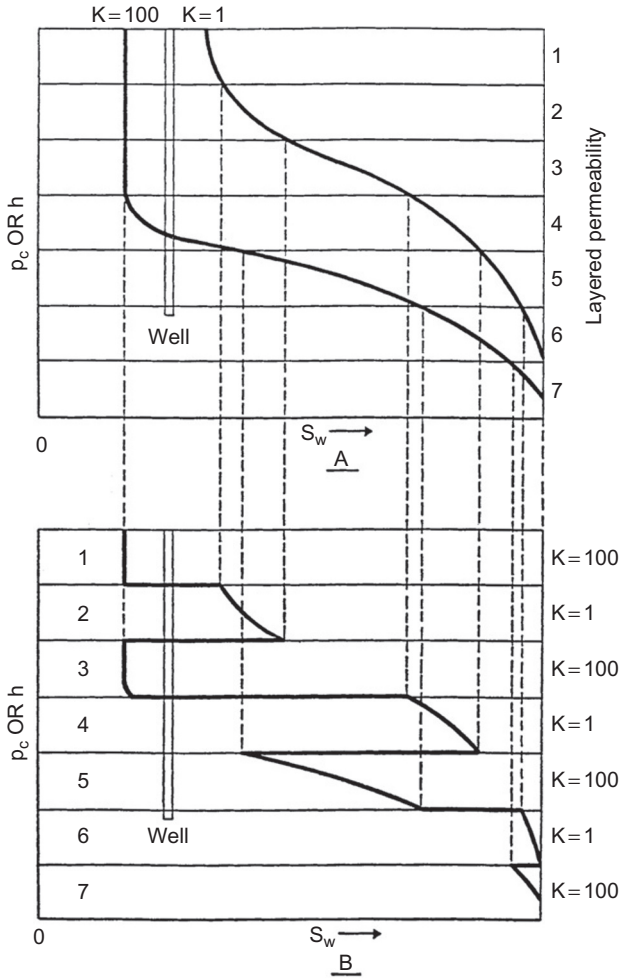


FIGURE 4-15 Effect of permeability on water saturation profile. (After Cole, F., 1969).

Example 4-6

A four-layer oil reservoir is characterized by a set of reservoir capillary pressure-saturation curves as shown in Figure 4-16. The following additional data are also available.

Layer	Depth, ft	Permeability, md
1	4000–4010	80
2	4010–4020	100
3	4020–4035	70
4	4035–4060	90